PERGAMON

Journal of Quantitative Spectroscopy & Radiative Transfer 82 (2003) 491–504

Journal of Quantitative Spectroscopy & Radiative Transfer

www.elsevier.com/locate/jqsrt

Ultraviolet and visible absorption cross-sections for HITRAN

Johannes Orphal[a,*], Kelly Chance[b]

[a] *Laboratoire de Photophysique Moléculaire, CNRS UPR-Universite de Paris-Sud Moleculaire, Bât. 350 centre d'Orsay, Orsay, Cedex 91405, France*

[b] *Harvard-Smithsonian Center for Astrophysics, Cambridge, MA 02138, USA*

Received 31 January 2003; received in revised form 5 March 2003; accepted 8 March 2003

Abstract

Ultraviolet-visible absorption cross-sections are important reference data for remote sensing of atmospheric trace gases including O_3, NO_2, BrO, H_2CO, OClO, SO_2, and NO_3 using optical instruments. In this paper, the reference absorption cross-sections for the HITRAN database are presented and needs for future improvements are addressed.

Keywords: Cross-section; Ultraviolet visible; Remote sensing; Trace gases; Atmosphere

1. Introduction

A number of ultraviolet-visible (UV-Vis) remote-sensing instruments now operate, or are planned, for monitoring the Earth's atmosphere. These include instruments measuring backscattered or reflected sunlight from ground or balloon- and space-borne platforms, in solar and lunar occultation, and in limb-scattered radiation [1–7]. In this spectral region (ca 200–800 nm), limited by the transition to the vacuum ultraviolet and to the near-infrared regions on the short- and long-wavelength sides, many atmospheric molecules have characteristic absorption features (see Fig. 1) that are used for detection and concentration determination [8–10]. For this purpose, accurate reference absorption spectra for each species from laboratory work are indispensable.

While existing UV-Vis databases [11,12] mainly focus on cross-sections for photochemical modeling of the atmosphere, the HITRAN database provides reference data for optical detection, so that, in addition to quantitative accuracy, instrumental issues such as spectral resolution and spectral

* Corresponding author. Tel.: +33-1-6915-752886; fax: +33-1-6915-753055.
E-mail address: johannes.orphal@ppm.u-psud.fr (J. Orphal).

0022-4073/03/$ - see front matter © 2003 Elsevier Ltd. All rights reserved.
doi:10.1016/S0022-4073(03)00173-0

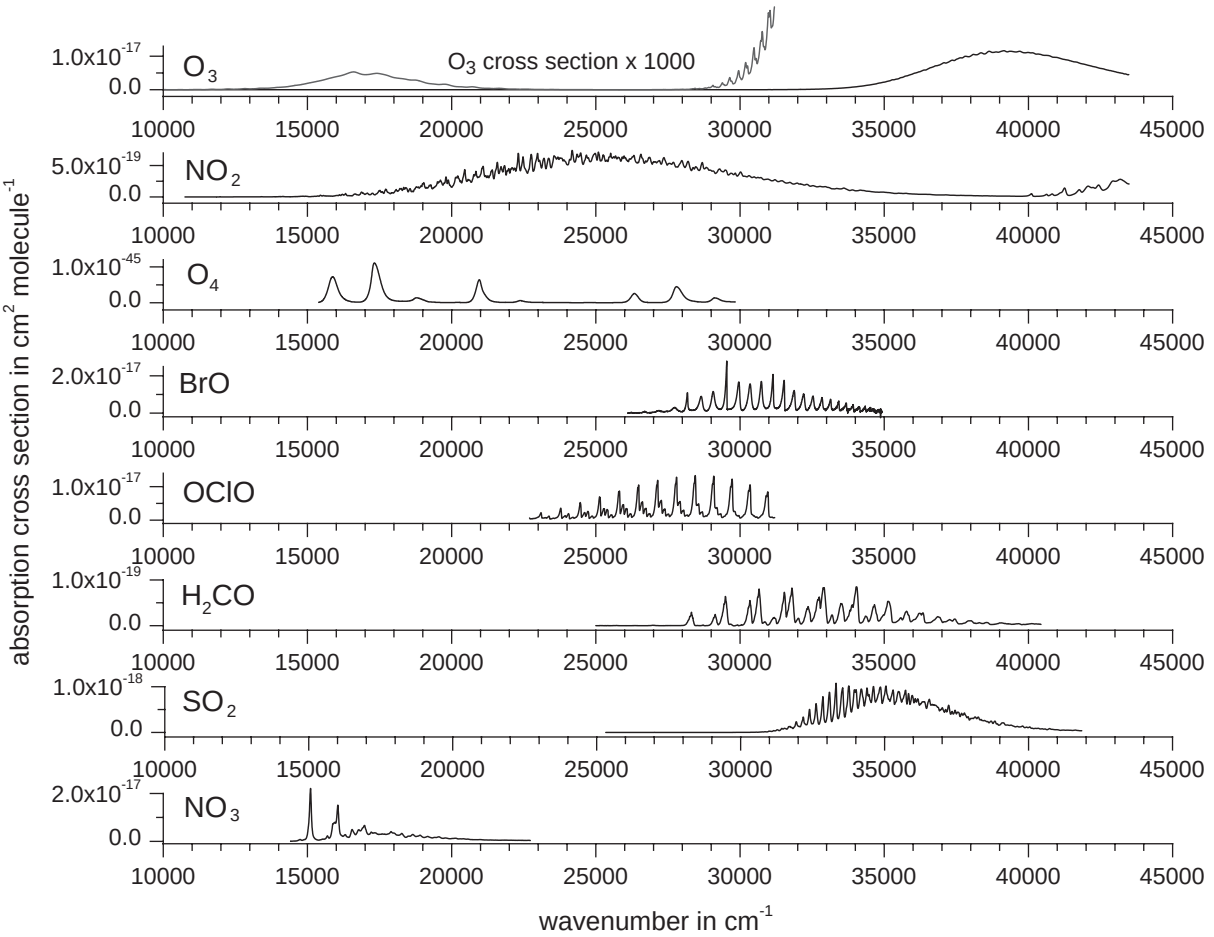

Fig. 1. Overview of the absorption cross-sections of the species in HITRAN. The units for O_4 are cm^5 $molecule^{-2}$; the absorption scales quadratically with pressure.

calibration become very important. Therefore, the HITRAN database contains reference cross-sections for the most important atmospheric absorbers that have been selected taking these criteria into account. Since, at present, theoretical models are not generally available to predict these spectra and their variation with temperature and pressure, it is necessary to provide absorption cross-sections for each species at different temperatures (in the 200–300 K range) and pressures (1–1000 mbar) where available, and empirical models to interpolate these cross-sections to intermediate values of temperature and pressure.

Many cross-section data available in the literature suffer from insufficient spectral resolution, i.e., the molecular absorption structures are narrower than the instrumental line shape of the spectrometer used for recording the data. In general, these data are only useful for atmospheric remote sensing after careful convolution of the atmospheric spectra with an appropriate transfer function, in order to minimize artifacts during the data reduction. In addition, spectral calibration using secondary wavelength

standards such as the visible iodine absorption lines [14–16] is frequently lacking. When atomic emission lines are used for calibration, the number of lines is often too low to account for systematic errors in the wavelength scale (curvature of the focal plane when using diode arrays, non-linearities in the drive for grating spectrometers). Only recently have a number of new spectra recorded with high-resolution Fourier-transform spectroscopy (FTS) been published (see e.g., [17] and references therein), providing additional information on the high-resolution structure of the spectra (in particular for very dense spectra like those of NO_2) and on the absolute wavelength calibration of the molecular cross-sections.

In the remainder of this paper we will first give a few definitions concerning cross-sections, air–vacuum correction, and wavelength calibration. We will then briefly discuss the available reference data for each molecule and explain the choices for HITRAN. Finally, we will address needs for future improvements.

2. Molecular absorption cross-sections

In the following, the molecular absorption cross-section σ is defined by [13]

$$\sigma(\lambda, T) = -\ln[I(\lambda, T, \rho)/I_0(\lambda)]/(\rho \times l),$$

where λ is the vacuum wavelength in nm, T is the absolute temperature in K, ρ is the molecular number density (or concentration) in molecules cm^{-3}, and l is the absorption path length in cm. The measured quantities are $I_0(\lambda)$, which is a spectrum recorded with no absorbing molecules in the light path (white light source spectrum), and $I(\lambda, T, \rho)$, which is a spectrum recorded using a certain concentration ρ of molecules at a given temperature T, both with the same absorption path l.

Cross-sections are often given in units of cm^2 $molecule^{-1}$ as a function of wavelength (nm) but are increasingly given as a function of wave number (cm^{-1}), in particular for spectra recorded using high-resolution FTS.

HITRAN cross-section files are standardized to even wave number increments. In those cases where the data are provided on a wavelength scale, the data are interpolated to a wave number grid for the standard database, and the data versus wavelength provided in supplementary files.

3. Air–vacuum correction and wavelength calibration

The refractive index of air leads to a difference between wavelengths measured in air and in vacuum. Therefore, it is essential to indicate at what conditions the cross-section spectra were recorded in the laboratory. In addition to that, the conversion of vacuum wavelengths into air wavelengths (and vice versa) is often performed using different formulae. In case of such a wavelength correction, it must be clear what formula has been used. For many years, the formulae of Edlén [18,19] have been used. Corrections in the present data are made using the second formula of Edlén [19]

$$\lambda_{vac} = \lambda_{air} \times (1.0000834213 + 2.40603 \times 10^{-2}/(130\text{–}10^6/\lambda_{air}^2) + 1.5997 \times 10^{-4}/(38.9\text{–}10^6/\lambda_{air}^2),$$

which is valid for standard conditions (dry air, room temperature, ambient pressure). The variation for slightly different conditions (humidity, temperature) is negligible for present atmospheric studies. For future conversions, we now recommend the use of Eq. (29) of Ref. [20]; however, the differences are sufficiently small that it is not necessary to reconvert the present spectra.

In the past, atomic emission lines, mostly from Hg and Cd, have been used for absolute wavelength calibration of spectra [21]. A difficulty is that these lines are rather sparsely scattered over the spectral range 240–800 nm, with gaps of up to several tens of nm. In many cases, due to this and to the limited spectral resolution of the instruments used, the absolute wavelength uncertainty of the reference spectra can be limited to several tenths of a nm, except for a few works where high-resolution grating spectrometers were used. For reference spectra recorded by FTS, the absolute wavelength uncertainty is usually much better, often better than 0.001 nm, but absolute calibration depends on the optical alignment of the instrument [22] and needs to be validated or improved using secondary wavelength standards as is usual in the infrared [23]. In the UV-visible, the use of molecular iodine absorption lines whose line positions are known to about 10^{-6} relative uncertainty [14–16], or other molecular absorbers like O_2 whose line positions are known with comparable accuracy [24–26] is recommended. Note that the emission spectra of Pt/Cr-Ne hollow cathode lamps have been measured in the UV-visible and near-infrared using high-resolution FTS [27,28] so that the lines of atomic Pt, Cr and Ne are also accurate standards in the 240–800 nm region (relative uncertainty of several parts in 10^7). These or similar lamps are also used for absolute wavelength calibration of space-borne optical instruments on the Hubble space telescope [29], the GOME instrument onboard ERS-2 [30], the SCIAMACHY instrument onboard ENVISAT-1 [31] and the GOME-2 instruments currently being prepared for the MetOp missions [32].

4. Cross-sections in HITRAN

4.1. O_3, ozone

Ozone shows absorption in the entire UV-Vis region [33,34], from the very strong Hartley band in the UV, through the much weaker Huggins and Chappuis bands in the near-UV and visible, to the very weak Wulf bands in the near-infrared part of the spectrum. Both the Huggins and Chappuis bands are frequently used for atmospheric remote sensing of ozone [35]. The large temperature dependence of the Huggins bands, due to the onset of vibrational hot band structure, has been proposed and used in distinguishing between stratospheric and tropospheric O_3 in nadir measurements from space [36]. A recent review [37] shows that, although many laboratory measurements have been reported in the past, the current knowledge of absolute absorption cross-sections of O_3 is only accurate to a few percent, except for a few selected wavelengths where the accuracy is 1–2% or better (in particular at 253.65 nm, the wavelength of one of the strongest atomic mercury emission lines) and where the variation of the ozone absorption with respect to wavelength shifts or spectral resolution is much smaller.

In the Hartley band (ca 200–320 nm), many laboratory data show agreement to 1–2%, in particular those of Bass and Paur [38] and Brion et al. [39] except for small wavelength shifts in the Bass and Paur data. This region is important for O_3 profile retrieval from space instruments such as GOME, which use full radiometric information. There is a general agreement that the

cross-section at 253.65 nm shows a small increase of about 1% between 293 and 203 K, as first observed by Molina and Molina [40]. The 253.65 nm cross-section of Hearn [41] measured in 1961 (1.147×10^{-17} cm^2 molecule^{-1}), in excellent agreement with many other measurements, is still the primary standard for international agencies like the International Ozone Committee (that recommends standards for the Dobson and Brewer networks) or the Bureau International des Poids et Mesures (that recommends standards for surface ozone measurements). Note that the currently available digital data [42] of Bass and Paur were calibrated to this standard after taking into account the small variation of the cross-section at 253.65 nm with temperature.

The agreement between different laboratory measurements is very good (about 1–2%) for the data of Bass and Paur [36], Brion et al. [37] and Burrows et al. [43] in the region of the Huggins bands (ca 320–350 nm), where the spectrum is extremely dependent on temperature. Note, however, that the data of Bass and Paur had to be wavelength corrected using high-resolution FTS data [44] and that they do not cover wavelengths above 343 nm. The cross-sections of Burrows et al. [43] have very high signal-to-noise ratios but were recorded with a spectral resolution that is not sufficiently high to resolve fully the spectral structures of ozone in the Huggins bands. The cross-sections of Brion et al. [37] show less noise than those of Bass and Paur [36] and more accurate wavelength calibration but do not cover temperatures below 218 K.

The agreement between different laboratory data is less satisfactory in the Chappuis band (about 400–700 nm) where systematic differences of 2–5% are observed, in particular in the region below 500 nm [37] that is frequently used for atmospheric O_3 retrievals. Also, there are only a few measurements that yield the ratio between the O_3 absorption cross-sections in the Huggins and Chappuis bands, and they show variations of 3–4%.

There are only few measurements of the O_3 absorption cross-sections in the Wulf bands (above 700 nm), although this region is important because of the O_2 *A* band around 762 nm that is used for determination of cloud parameters [45], so that correction for the atmospheric O_3 absorption is required [46].

There have been several intercomparisons [47–49] of O_3 absorption coefficients in the ultraviolet and mid-infrared showing agreement to better than 5%, although two studies [47,49] show small but systematic discrepancies that remain currently unexplained, since in both regions the agreement between other studies is better [37,50]. Work is currently in progress to increase the accuracy of these measurements and to extend the range to the important Huggins and Chappuis bands [51–53].

The temperature-dependent ozone cross-sections of Bass and Paur [38] are selected for inclusion in HITRAN, in accordance with the recommendation of Ref. [37]. They are converted to vacuum wavelengths using the Edlén 1966 formula [19] and shifted in wavelength by a further 0.015 nm, from fitting to FTS measurements [56]. The final wavelength uncertainty is 0.040 nm.

4.2. *NO_2, nitrogen dioxide*

The NO_2 absorption covers the entire UV-Vis and near-infrared regions. Its peak absorption cross-sections are over an order of magnitude weaker than those of O_3, so that NO_2 shows much smaller absorption in atmospheric spectra with comparable atmospheric concentration [4]. The absorption spectrum of NO_2 has very narrow spectral structures that show variations both with temperature and with pressure [54–56]. Therefore, the NO_2 cross-sections have to be recorded at high spectral

resolution and at representative total pressures. The temperature dependence of the cross-sections is potentially useful for the separation of stratospheric and tropospheric NO_2 absorption in atmospheric spectra [57]. Note that only the cross-section measurements of Frost et al. [58] and of Bogumil et al. [59] extend to temperatures below 220 K.

A recent review [54] concluded that the FTS measurements of Vandaele et al. [60,61] at two temperatures (293 and 220 K) are in excellent agreement with many other laboratory data, and show only very small problems with respect to wavelength calibration errors and baseline drifts. In particular, these data are in very good agreement (of 1–2%) with the measurements of Mérienne et al. [62] and of Yoshino et al. [63]. If required, the cross-sections can be interpolated by a linear model to obtain values at intermediate temperatures [54].

Very recently, an empirical model based upon an exhaustive compilation of different experimental data has been proposed [64] that predicts the variation of the NO_2 cross-sections with temperature and pressure, reproducing the experimental data to better than 10%. The overall uncertainty of the NO_2 cross-sections of Vandaele et al. at 298 K [60] and 220 K [61] is estimated to be 2% or less. The Vandaele et al. cross-sections are included in HITRAN. Note that these do not include the variation of the NO_2 spectrum with total pressure.

4.3. O_4, oxygen dimer/O_2–O_2, collision-induced absorption

The theoretical basis for the absorption due to the so-called oxygen dimer is still not entirely established; there is a major contribution from collision-induced absorption while at low temperatures a weakly bound complex is formed. There are several sets of absorption cross-sections available in the literature (see [65,66] and references therein), since the absorptions of O_4/O_2–O_2 must be taken into account in the retrieval of other species [4]. These features have also been used for air mass factor determinations [67,68] and are potentially useful for cloud detection [69]. Recently, the first measurements of these absorptions at atmospheric pressures using Cavity Ring-Down spectroscopy have been published [70]. For HITRAN, the cross-sections of Greenblatt et al. [65], corrected to vacuum wavelengths using Edlén [19] have been selected, since they show the smallest residuals in recent analyses of atmospheric spectra [67,68] (Fig. 1 and Table 1).

4.4. BrO, bromine monoxide

BrO is measured in the UV-Vis using the strong $A^2\Pi_{3/2} \leftarrow X^2\Pi_{3/2}$ vibronic bands between 300–400 nm [4]. Most of these bands are heavily broadened by predissociation, except for the 4-0, 7-0, and 12-0 bands. These have been studied in the past by high-resolution spectroscopy, resolving the rotational structure [71,72]. The BrO cross-sections show a significant variation with temperature due to the change in thermal populations of the lower states.

For remote sensing, two sets of measurements are currently used: the cross-sections of Wahner et al. [73] recorded with a grating spectrometer at two temperatures (223 and 293 K) and the spectra of Wilmouth et al. [74] recorded with a high-resolution FTS at two temperatures (228 and 293 K). The cross-sections of Wahner et al. were calibrated to absolute cross-sections using chemical methods, whereas Wilmouth et al. obtained absolute cross-sections by scaling their data using previous absolute measurements.

Table 1
Ultraviolet-visible cross-sections in HITRAN

Molecule	Reference	T range (K)	Spectral range (cm^{-1})	Resolution (cm^{-1})	Wave number accuracy (cm^{-1})
O_3	Bass and Paur [38][a]	203–298	29154–40816	ca 3.0[b]	ca. 3.5[c]
NO_2	Vandaele et al. [60,61]	220–298	10000–42000	2.0	0.08
O_4	Greenblatt et al. [65]	196–298	8797–29833	ca 5–50[b]	ca 1.5–18[b]
BrO	Wilmouth et al. [74]	223, 298	26000–34918	10.0	0.2
OClO	Kromminga et al. [82]	203–298	22988–30770	1.0	0.01
H_2CO	Cantrell et al. [87]	296	25974–33300	1.0	ca 0.02[b]
SO_2	Rufus et al. [92]	295	30770–45455	0.06–0.48[d]	0.2
NO_3	Yokelson et al. [95]	200–298	13888–22727	ca 6.0[b]	0.02[e]

[a] Including the variation of the cross-section at 265 nm with temperature.
[b] Approximate value, original data were recorded as a function of wavelengths.
[c] After recalibration based on Fourier-transform spectra of Voigt et al. [56], see text. The shift is 1.75 cm^{-1} (0.015 nm) to the red.
[d] Depending upon region of the spectrum.
[e] After recalibration based on Fourier-transform spectra of Orphal et al. [96], see text. The shift is 6.27 cm^{-1} (0.275 nm) to the red.

A recent intercomparison of BrO field measurements by Aliwell et al. [75] demonstrated that one of the main potential sources for systematic errors in the retrieved BrO concentrations is the uncertainty in the wavelength calibration of the reference data (up to 30%). It is known that the cross-section data of Wahner et al. have wavelength errors of several tenths of a nm. Also, the data of Wahner et al. were recorded with a spectral resolution that is larger than the spectral structures of BrO although this contributes less to systematic errors than the wavelength calibration [75]. Very recently, new FTS measurements at five temperatures down to 203 K have been recorded [76], and the BrO cross-sections and their temperature dependence are currently being modeled using quantum-mechanical calculations including the effects of predissociation [77].

The overall uncertainty of the BrO cross-sections of Wilmouth et al. [74] is given as 8% for absolute values and 11% for the differential structures. These BrO data, for temperatures of 223 and 298 K are included in HITRAN.

4.5. OClO, chlorine dioxide

OClO has a well-known strong electronic band system extending from the visible to near-ultraviolet (about 300–500 nm) with very narrow (rotationally resolved) features [78,79] that show increasing widths due to predissociation towards shorter wavelengths [80]. The state of the data for OClO is similar to that of BrO. For more than a decade, the cross-sections of Wahner et al. [81], recorded with a grating spectrometer at several temperatures between 203 and 293 K, have been used for atmospheric detection of OClO. Because of errors in the wavelength calibration and the limited spectral resolution of the data of Wahner et al., new OClO cross-sections have been recently measured using high-resolution FTS [82]. These cross-sections are in good agreement with several other laboratory measurements but about 10% lower than the data of Wahner et al. The overall uncertain-

ties of the OClO cross-sections of Kromminga et al. [82] are less than 9%. These data are included in HITRAN.

4.6. H_2CO, formaldehyde

H_2CO is one of the most important products of the oxidation of volatile organic compounds in the troposphere. Tropospheric column densities can be measured from space using the electronic bands in the region above 300 nm [83–86]. Cantrell et al. [87] have measured absorption cross-sections at temperatures of 223–293 K using FTS, with intensity errors of 5% at the higher temperature (characteristic of the dominantly tropospheric H_2CO). Cantrell et al. provide a linear temperature parameterization valid over the range of stratospheric and tropospheric temperatures. Additional errors from the use of cross-sections at a single temperature may be as much as 5% (the integral of the cross-sections changes by 5% going from 300 to 270 K), for total errors of up to 7%. Meller and Moortgat [88] have provided accurate measurements of the temperature dependence of the cross-sections using a grating instrument with intensity errors better than 10%, a major contribution to the uncertainty being the polymerization of H_2CO even at low partial pressures. The data of Cantrell et al. are included in the HITRAN database at several temperatures. The temperature parameterization is included in an auxiliary file.

4.7. SO_2, sulfur dioxide

SO_2 has a pronounced band spectrum in the ultraviolet that has very sharp rotational structures visible only at high spectral resolution [89]. However, there is only one recent study of absorption spectra of SO_2 at temperatures other than room temperature [90], 203–293 K, using the cross-sections of Vandaele et al. [89] at 293 K for absolute calibration. The wavelength accuracy of the Vandaele et al. data is about 0.01 nm, and it shows better than 5% agreement compared to previous measurements at room temperature [91]. A recent study by Rufus et al. [92] provides accurate cross-sections at high spectral resolution and very high wavelength accuracy (< 0.001 nm) at 295 K, covering the spectral range employed for atmospheric measurements, with 5% accurate intensities. These data are included in HITRAN.

4.8. NO_3, nitrogen trioxide

The NO_3 radical is an important species in tropospheric chemistry. It shows a pronounced diurnal cycle due to its high absorption in the visible leading to rapid photolysis by sunlight [93]. It has not yet been detected in satellite data. The strongest absorption feature of NO_3, near 662 nm, increases significantly in intensity at lower temperatures while keeping the same spectral shape, due to dominant predissociation [94,95]. The NO_3 spectrum at room temperature was recently calibrated in wavelength using FTS and a theoretical expression for the temperature dependence of the 662 nm band was given [96]. The agreement in relative cross-sections among the most recent measurements [94–96] is excellent. However, the data from these studies differ in spectral resolution, wavelength calibration, and absolute values of the cross-sections. The data of Yokelson et al. [95], with the wavelength correction of Orphal et al. [96] are included in HITRAN. The intensities are accurate to at least 10%.

4.9. ClO, chlorine monoxide

The electronic spectrum of ClO in the ultraviolet has long been known and was accurately modeled (Franck–Condon factors and rotational constants) long before atmospheric detection was an issue [97]. There have been several studies of absolute absorption cross-sections and their temperature dependence (see [98,99] and references therein). A model that successfully reproduces all available experimental data was recently proposed [100]. The accuracy of the absolute cross-sections of ClO is estimated to be better than 10%. Despite the importance of ClO in stratospheric chemistry, useful stratospheric measurements have not yet been made using the UV spectrum because it is heavily masked by the strong O_3 absorption in the Hartley band. Some long-path tropospheric measurements under highly enhanced concentrations have been made. ClO is not yet included in HITRAN.

4.10. HONO, nitrous acid

The photolysis of HONO in the near UV is one of the most important sources of OH in the troposphere. However, its chemical sources are still not perfectly understood [10,101]. HONO is currently measured by long-path tropospheric DOAS [4] and its cross-sections are known to better than 10% (see [102] and references therein). HONO is not yet included in HITRAN.

4.11. Organic molecules in the UV

A number of aromatic molecules show characteristic absorption in the ultraviolet [4] and can therefore be measured using long-path tropospheric spectroscopy [103,104]. Although there have been recent measurements of some species, including glyoxal [105], future work is required to assess their accuracy and to provide clear recommendations for future inclusion in HITRAN.

5. Needs for future improvements

The overwhelming need for atmospheric measurements in the UV-Vis is to obtain improved cross-sections of ozone using FTS measurements [106]. Wavelength coverage of 240–1000 nm is required, at 0.01 nm spectral resolution or better. Absolute intensities should be accurate to at least 2% through the Hartley–Huggins and Chappuis bands (relative to the band maxima). Vacuum wavelength accuracy should be better than 0.001 nm, reflecting the accuracy to which atmospheric spectra can be calibrated using correlation with the Fraunhofer spectrum [107]. Measurements should be made over the 200–300 K temperature range. Particular care has to be paid to avoid baseline uncertainties which are a major source of systematic errors in such measurements [37].

An additional high-priority need is for an extraterrestrial solar reference spectrum with similar characteristics [106]. This will provide for accurate wavelength calibration of field spectra, including satellite spectra [107], improved characterization of the Ring effect, improved knowledge of instrument transfer functions, and correction of instrument undersampling [108]. It may also provide for improved modeling of atmospheric photochemistry due to absorption of solar radiation in the regions of the Schumann–Runge and Herzberg systems of O_2 [109,110].

Acknowledgements

The authors wish to thank the many colleagues mentioned in this paper for making available their cross-section data in digital form. K. Chance was supported in this work by NASA and by internal funding from the Smithsonian Institution.

References

[1] McPeters RD, Krueger AJ, Bhartia PK, Herman JR. Earth probe total ozone mapping spectrometer (TOMS) data products user's guide. NASA Reference Publication 1998-206895, 1998.
[2] SAGE III Algorithm Team. The SAGE III algorithm theoretical baseline document. NASA LARC, 2000.
[3] Hudson RD, Planet WG, editors. Handbook for Dobson Ozone Data Re-evaluation, WMO Global Ozone Research and Monitoring Project, Report No. 29, WMO/TD-No. 597, 1993.
[4] Platt U. Modern methods of the measurement of atmospheric trace gases. Phys Chem Chem Phys 1999;1:5409–15.
[5] Ferlemann F, Bauer N, Harder H, Osterkamp H, Perner D, Platt U, Schneider M, Vradelis P, Pfeilsticker K. A new DOAS-instrument for stratospheric balloon-borne trace gas studies. Appl Opt 2000;39:2377–86.
[6] Burrows JP, Weber M, Buchwitz M, Rozanov V, Ladstätter-Weißenmayer A, Richter A, DeBeek R, Hoogen R, Bramstedt K, Eichmann K-U, Eisinger M. The global ozone monitoring experiment (GOME): mission concept and first scientific results. J Atmos Sci 1999;56:151–75.
[7] Bovensmann H, Burrows JP, Buchwitz M, Frerick J, Noël S, Rozanov VV, Chance KV, Goede APH. SCIAMACHY: mission objectives and measurements modes. J Atmos Sci 1999;56:127–50.
[8] Okabe H. Photochemistry of small molecules. New York: Wiley, 1978.
[9] Brasseur G, Solomon S. Aeronomy of the middle atmosphere. Dordrecht: D. Reidel, 1986.
[10] Finlayson-Pitts BJ, Pitts JN. Chemistry of the upper and lower atmosphere: theory, experiments, and applications. New York: Academic Press, 1999.
[11] DeMore WB, Sander SP, Golden DM, Hampson RF, Kurylo MJ, Howard CJ, Ravishankara AR, Kolb CE, Molina MJ. Chemical kinetics and photochemical data for use in stratospheric modeling, evaluation number 12, JPL Publ., 97-4, 1997.
[12] International Union of Pure and Applied Chemistry (IUPAC), Subcommittee on Gas Kinetic Data Evaluation, evaluated kinetic data, Basel, Switzerland, updated 16 July 2001. (Available at www.iupac-kinetic.ch.cam.ac.uk.)
[13] Thorne AP, Litzen U, Johansson S. Spectrophysics: principles and applications. Berlin: Springer, 1999.
[14] Gerstenkorn S, Luc P. Atlas du spectre d'absorption de la molécule d'iode, vol. 1–4, CNRS, Laboratoire Aimé Cotton, 1978–1982.
[15] Bodermann B, Klug M, Winkelhoff U, Knöckel H, Tiemann E. Precise frequency measurements of I_2 lines in the near infrared by Rb reference line. Eur Phys J D 2000;11:213–25.
[16] Xu SC, van Dierendonck R, Hogervorst W, Ubachs W. A dense grid of reference iodine lines for optical frequency calibration in the range 595–655 nm. J Mol Spectrosc 2000;201:256–66.
[17] Orphal J, Bogumil K, Dehn A, Deters B, Dreher S, Fleischmann OC, Hartmann M, Himmelmann S, Homann T, Kromminga H, Spietz P, Türk A, Vogel A, Voigt S, Burrows JP. Laboratory spectroscopy in support of UV-visible remote-sensing of the atmosphere. In: Pandalai SG, editor. Recent research developments in physical chemistry, vol. 6. Trivandrum: Transworld Research Network, 2002. p. 15–34.
[18] Edlén B. The dispersion of standard air. J Opt Soc Am 1953;43:339–44.
[19] Edlén B. The refractive index of air. Metrologia 1966;2:71–80.
[20] Bodhaine BA, Wood NB, Dutton EG, Slusser JR. On Rayleigh optical depth calculations. J Atmos Oceanic Technol 1999;16:1854–61.
[21] NIST Atomic Spectra Database, NIST Standard Reference Database 78, 1999. Available at http://physics.nist.gov/PhysRefData/ASD1/nist_atomic_spectra.html.
[22] Davis SP, Abrams MC, Brault JW. Fourier transform spectrometry. New York: Academic Press, 2000.
[23] Guelachvili G, et al. High-resolution wavenumber standards for the infrared. Pure Appl Chem 1996;68:192–208.

[24] O'Brien LC, Cao H, O'Brien JJ. Molecular constants for the v=0, $b^1\Sigma_g^+$ excited state of O_2: improved values derived from measurements of the oxygen A-band using intracavity laser spectroscopy. J Mol Spectrosc 2001;207:99–103.
[25] Brown LR, Plymate C. Experimental line parameters of the oxygen *A* band at 760 nm. J Mol Spectrosc 2000;199: 166–79.
[26] Schermaul R, Learner RCM. Precise line parameters and transition probability of the atmospheric *A* band of molecular oxygen $^{16}O_2$. JQSRT 1999;61:781–94.
[27] Murray JE, Atlas of the spectrum of a platinum/chromium/neon hollow-cathode reference lamp in the region 240–790 nm. Final Report to ESA, John Wheaton Associates, London, 1994.
[28] Orphal J, Voigt S, Burrows JP. High-resolution Fourier-transform spectra of a Pt/Cr-Ne hollow-cathode emission lamp between 780–2500 nm. Technical Report for TPD/TNO (Delft), IUP, Bremen, 1997.
[29] Kriss GA, Hartig GF, Armus L, Blair WP, Caganoff S, Dressel L. Astrophys J 1991;377:L13.
[30] GOME Users Manual, ESA Special Publication SP-1182, ESTEC, Noordwijk, 1995.
[31] SCIAMACHY PFM calibration results review data package, TPD-TNO, Delft, 1999.
[32] Callies J, Corpaccioli E, Eisinger M, Hahne A, Lefebvre A. GOME-2—Metop's second-generation sensor for operational ozone monitoring. ESA Bulletin 2000;102:28–36.
[33] Steinfeld JI, Adler-Golden SM, Gallagher JW. Critical survey of data on the spectroscopy and kinetics of ozone in the mesosphere and thermosphere. J Phys Chem Ref Data 1987;16:911–51.
[34] Bacis R, Bouvier AJ, Flaud J-M. The ozone molecule: electronic spectroscopy. Spectrochim Acta A 1998;54: 17–34.
[35] Grant WB, editor. Ozone measuring instruments for the stratosphere. Collected works in optics, vol. 1. Washington, DC: Optical Society of America, 1989.
[36] Chance KV, Burrows JP, Perner D, Schneider W. Satellite measurements of atmospheric ozone profiles, including tropospheric ozone, from UV/visible measurements in the nadir geometry: a potential method to retrieve tropospheric ozone. JQSRT 1997;57:467–76.
[37] Orphal J. A critical review of the absorption cross-sections of O_3 and NO_2 in the 240–790 nm region. Part I: Ozone, ESA Technical Note MO-TN-ESA-GO-0302, 2002.
[38] Bass AM, Paur RJ. Absorption cross-sections for ozone: the temperature dependence. J Photochem 1981;17:141;
Bass AM, Paur RJ. The ultraviolet cross-sections of ozone: I the measurements. In: Zerefos CS, Ghazi A, editors. Atmospheric ozone. Dordrecht: Reidel D, 1985. p. 606–10;
Bass AM, Paur RJ. The ultraviolet cross-sections of ozone: II results and temperature dependence. In: Zerefos CS, Ghazi A, editors. Atmospheric ozone. Dordrecht: Reidel D, 1985. p. 611–6.
[39] Brion J, Chakir A, Daumont D, Malicet J, Parisse C. High-resolution laboratory cross-sections of O_3: temperature effect. Chem Phys Lett 1993;213: 610–2;
Malicet J, Daumont D, Charbonnier J, Parisse C, Chakir A, Brion J. Ozone UV spectroscopy II: absorption cross sections and temperature dependence. J Atm Chem 1995;21:263–73.
[40] Molina LT, Molina MJ. Absolute absorption cross sections of ozone in the 185- to 350-nm wavelength range. J Geophys Res D 1986;91:14501–8.
[41] Hearn AG. The absorption of ozone in the ultraviolet and visible regions of the spectrum. Proc Phys Soc 1961;78: 932–40.
[42] McPeters RD, Gleason J, Chance KV. Personal communication, 1999.
[43] Burrows JP, Richter A, Dehn A, Deters B, Himmelmann S, Voigt S, Orphal J. Atmospheric remote-sensing reference data from GOME: 2. Temperature-dependent absorption cross sections of O_3 in the 231–794 nm range. JQSRT 1999;61:509–17.
[44] Voigt S, Orphal J, Burrows JP. The temperature- and pressure-dependence of the absorption cross-sections of NO_2 in the 250–800 nm region measured by Fourier-transform spectroscopy. J Photochem Photobiol A: Chem 2002;149:1 –7.
[45] Kuze A, Chance KV. Analysis of cloud top height and cloud coverage from satellites using the O_2 *A* and *B* bands. J Geophys Res D 1994;99:14481–91.
[46] Kurosu TP, Chance KV, Yokota T, Sasano Y. Polar stratospheric cloud detection from the ILAS instrument. In: Sasano Y, Wang J, Hayasaka T, editors. Optical remote sensing of the atmosphere and clouds, vol. II. Proc SPIE 2001;4150:68–75.

[47] Pickett HM, Peterson DB, Margolis JS. Absolute absorption of ozone in the mid infrared. J Geophys Res 1992;97:20787–93.

[48] DeBacker-Barilly MR, Barbe A. Absolute intensities of the 10-μm bands of $^{16}O_3$. J Mol Spectrosc 2001;205: 43–53.

[49] Smith MAH, Malathy Devi V, Benner DC, Rinsland CP. Absolute intensities of $^{16}O_3$ lines in the 9–11 μm region. J Geophys Res 2001;106:9909–21.

[50] Flaud J-M, Wagner G, Birk M, Camy-Peyret C, Claveau C, De Backer-Barilly MR, Barbe A, Piccolo C. The ozone absorption around 10 μm. J Geophys Res 2003, in press.

[51] Picquet-Varrault B. Personal communication, 2002.

[52] Carleer M. Personal communication, 2002.

[53] Spietz P. Personal communication, 2003.

[54] Orphal J. A critical review of the Absorption Cross-Sections of O_3 and NO_2 in the 240–790 nm Region. Part II: Nitrogen Dioxide, ESA Technical Note MO-TN-ESA-GO-0302, 2002.

[55] Burrows JP, Dehn A, Deters B, Himmelmann S, Richter A, Voigt S, Orphal J. Atmospheric remote-sensing reference data from GOME: 1. Temperature-dependent absorption cross sections of NO_2 in the 231–794 nm range. JQSRT 1998;60:1025–31.

[56] Voigt S, Orphal J, Burrows JP. The temperature- and pressure-dependence of the absorption cross-sections of NO_2 in the 250–800 nm region measured by Fourier-transform spectroscopy. J Photochem Photobiol A: Chem 2002;149: 1–7.

[57] Richter A, Burrows JP. Retrieval of tropospheric NO_2 from GOME measurements. Adv Space Res 2002;29: 1673–83.

[58] Frost GJ, Goss LM, Vaida V. Measurements of high resolution ultraviolet-visible absorption cross sections at stratospheric temperatures. 1. Nitrogen dioxide. J Geophys Res 1996;101:3869–77.

[59] Bogumil K, Orphal J, Homann T, Voigt S, Spietz P, Fleischmann OC, Vogel A, Hartmann M, Bovensmann H, Frerick J, Burrows JP. Measurements of molecular absorption spectra with the SCIAMACHY pre-flight model: instrument characterization and reference data for atmospheric remote-sensing in the 230–2380 nm region. J Photochem Photobiol A: Chem 2003;157:167–84.

[60] Vandaele AC, Hermans C, Simon PC, Van Roozendael M, Guilmot JM, Carleer M, Colin R. Fourier transform measurement of NO_2 absorption cross-sections in the visible range at room temperature. J Atm Chem 1996;25:289 –305.

[61] Vandaele A-C, Hermans C, Simon PC, Carleer M, Colin R, Fally S, Mérienne M-F, Jenouvrier A, Coquart B. Measurements of the NO_2 absorption cross-section from 42000 cm^{-1} to 10000 cm^{-1} (238–1000 nm) at 220 K and 294 K. JQSRT 1998;59:171–84.

[62] Mérienne MF, Jenouvrier A, Coquart B. The NO_2 absorption spectrum. I: absorption cross-sections at ambient temperature in the 300–500 nm region. J Atm Chem 1995;20:281–97;
Coquart B, Jenouvrier A, Mérienne MF. The NO_2 absorption spectrum. II: absorption cross-sections at low temperatures in the 400–500 nm region. J Atm Chem 1995;21:251–61;
Mérienne MF, Jenouvrier A, Coquart B. The NO_2 absorption spectrum. III: The 200–300 nm region at ambient temperature. J Atm Chem 1996;25:21–32;
Mérienne MF, Jenouvrier A, Coquart B, Lux JP. The NO_2 absorption spectrum. IV: The 200–400 nm region at 220 K. J Atm Chem 1997;27:219–32.

[63] Yoshino K, Esmond JR, Parkinson WH. High resolution absorption cross section measurements of NO_2 in the UV and visible region. Chem Phys 1997;221:169–74.

[64] Vandaele A-C, Hermans C, Fally S, Carleer M, Colin R, Merienne M-F, Jenouvrier A. High-resolution Fourier-transform measurement of the NO_2 visible and near-infrared absorption cross section: temperature and pressure effects. J Geophys Res 107(D18), 4348, 2002. doi:10.1029/2001JD000971.

[65] Greenblatt GD, Orlando JJ, Burkholder JB, Ravishankara AR. Absorption measurements of oxygen between 330 and 1140 nm. J Geophys Res 1990;95:18,577–82.

[66] Newnham DA, Ballard J. Visible absorption cross-sections and integrated absorption intensities of molecular oxygen (O_2 and O_4). J Geophys Res 1998;103:28,801–16.

[67] Pfeilsticker K, Bösch H, Camy-Peyret C, Fitzenberger R, Harder H, Osterkamp H. First atmospheric profile measurements of UV/visible O_4 absorption band intensities: implications for the spectroscopy, and the formation enthalpy of the O_2-O_2 dimer. Geophys Res Lett 2001;28:4595–8.
[68] Wagner T, von Friedeburg C, Wenig M, Otten C, Platt U. UV-visible observations of atmospheric O_4 absorptions using direct moonlight and zenith-scattered sunlight for clear-sky and cloudy sky conditions. J Geophys Res 2002, D10.1029/2001JD001026.
[69] Bhartia PK, editor. OMI Algorithm Theoretical Basis Document, vol. II. OMI Ozone products, 2001.
[70] Naus H, Ubachs W. Visible absorption bands of the $(O_2)_2$-collision complex at pressures below 760 Torr. Appl Opt 1999;38:3423–8.
[71] Durie RA, Ramsay DA. Can J Phys 1958;36:35.
[72] Wheeler MD, Newman SM, Ishiwata T, Kawasaki M, Orr-Ewing AJ. Cavity ring-down spectroscopy of the $A^2\Pi$-$X^2\Pi$ transition of BrO. Chem Phys Lett 1998;285:346–51.
[73] Wahner A, Ravishankara AR, Sander SP, Friedl RR. Absorption cross section of BrO between 312 and 385 nm at 298 and 223 K. Chem Phys Lett 1988;152:507–12.
[74] Wilmouth DM, Hanisco TF, Donahue NM, Anderson JG. Fourier transform ultraviolet spectroscopy of the $A^2\Pi_{3/2}$-$X^2\Pi_{3/2}$ transition of BrO. J Phys Chem 1999;103:8935–45.
[75] Aliwell SR, Van Roozendael M, Johnston PV, Richter A, Wagner T, Arlander DW, Burrows JP, Fish DJ, Jones RL, Tornkvist KK, Lambert JC, Pfeilsticker K, Pundt I. Analysis for BrO in zenith-sky spectra: an intercomparison exercise for analysis improvement. J Geophys Res 107(D14), 2002, doi:10.1029/2001JD000329.
[76] Fleischmann OC, Burrows JP, Orphal J. Ultraviolet absorption cross-sections of BrO measured by time-windowing Fourier transform spectroscopy. J Photochem Photobiol A: Chem, submitted for publication.
[77] Orphal J, Fellows CE. 2003, to be published.
[78] Coon JB, Ortiz E. The vibrational analysis of the 2700–4800 Å absorption system of ClO_2 and the vibrational constants of the associated electronic states. J Mol Spectrosc 1957;1:81–94.
[79] Hamada Y, Merer AJ, Michielsen S, Rice SA. Rotational analysis of bands at the long-wavelength end of the A^2A_2-X^2B_1 electronic transition of ClO_2. J Mol Spectrosc 1981;86:499–525.
[80] Michielsen S, Merer AJ, Rice SA, Novak FA, Freed KF, Hamada Y. A study of the rotational state dependence of predissociation of a polyatomic molecule: the case of ClO_2. J Chem Phys 1981;74:3089–101.
[81] Wahner A, Tyndall GS, Ravishankara AR. Absorption cross sections for OClO as a function of temperature in the wavelength range 240–480 nm. J Phys Chem 1987;91:2734–8.
[82] Kromminga H, Orphal J, Spietz P, Voigt S, Burrows JP. The temperature dependence (213–293 K) of the absorption cross-sections of OClO in the 340–450 nm region measured by Fourier-transform spectroscopy. J Photochem Photobiol A: Chem, 2003;157:149–60.
[83] Thomas W, Hegels E, Slijkhuis S, Spurr R, Chance K. Detection of biomass burning combustion products in southeast asia from backscatter data taken by the GOME spectrometer. Geophys Res Lett 1998;25:1317–20.
[84] Chance K, Palmer PI, Spurr RJD, Martin RV, Kurosu TP, Jacob DJ. Satellite observations of formaldehyde over North America from GOME. Geophys Res Lett 2000;27:3461–4.
[85] Palmer PI, Jacob DJ, Chance K, Martin RV, Spurr RJD, Kurosu TP, Bey I, Yantosca R, Fiore A, Li Q. Air mass factor formulation for spectroscopic measurements from satellites: application to formaldehyde retrievals from the global ozone monitoring experiment. J Geophys Res 2001;106:14,539–50.
[86] Palmer PI, Jacob DJ, Fiore AM, Martin RV, Chance K, Kurosu TP. Mapping isoprene emissions over North America using formaldehyde column observations from space. J Geophys Res 108(D6), 2003, doi:10.1029/2002JD002153.
[87] Cantrell CA, Davidson JA, McDaniel AH, Shetter RE, Calvert JG. Temperature-dependent formaldehyde cross sections in the near-ultraviolet spectral region. J Phys Chem 1990;94:3902–8.
[88] Meller R, Moortgat GK. Temperature dependence of the absorption cross sections of formaldehyde between 223 and 323 K in the wavelength range 225–375 nm. J Geophys Res 2000;105:7089–101.
[89] Vandaele AC, Simon PC, Guilmot JM, Carleer M, Colin R. SO_2 absorption cross section measurement in the UV using a Fourier transform spectrometer. J Geophys Res 1994;99:25,599–605.
[90] Bogumil K, Orphal J, Homann T, Voigt S, Spietz P, Fleischmann OC, Vogel A, Hartmann M, Bovensmann H, Frerick J, Burrows JP. Measurements of molecular absorption spectra with the SCIAMACHY pre-flight model: instrument characterization and reference data for atmospheric remote-sensing in the 230–2380 nm region. J Photochem Photobiol A: Chem 2003;157:167–84.

[91] Sprague KE, Joens JA. SO_2 absorption cross-section measurements from 320 to 405 nm. JQSRT 1995;53:349–52.
[92] Rufus J, Stark G, Smith PL, Pickering JC, Thorne AP. High resolution photoabsorption cross section measurements of SO_2, II: 220 to 325 nm at 295 K. J Geophys Res 2003, in press.
[93] Wayne RP, Barnes I, Biggs P, Burrows JP, Canosa-Mas CE, Hjorth L, Le Bras G, Moortgat GK, Perner D, Poulet G, Restelli G, Sidebottom H. The nitrate radical: Physics, chemistry, and the environment. Atmos Environ Part A 1991;25:1–206.
[94] Sander SP. Temperature dependence of the NO_3 absorption spectrum. J Phys Chem 1996;90:4135–42.
[95] Yokelson RJ, Burkholder JB, Fox RW, Talukdar RK, Ravishankara AR. Temperature dependence of the NO_3 absorption spectrum. J Phys Chem 1994;98:13,144–50.
[96] Orphal J, Fellows CE, Flaud P-M. The visible absorption spectrum of NO_3 measured by high-resolution Fourier-transform spectroscopy. J Geophys Res 108(D3), 2003, doi:10.1029/2002JD002489.
[97] Coxon JA. RKR Franck-Condon factors and absorption cross-sections for rotational transitions in the $A^2\Pi \leftarrow X^2\Pi$ system of ClO. J Photochem 197677;6:439–52.
[98] Sander SP, Friedl RR. Kinetics and product studies of the reaction ClO + BrO using flash photolysis-ultraviolet absorption. J Phys Chem 1989;93:4764–71.
[99] Simon FG, Schneider W, Moortgat GK, Burrows JP. A study of the ClO absorption cross-section between 240 and 310 nm and the kinetics of the self-reaction at 300 K. J Photochem Photobiol A: Chem 1990;55:1–23.
[100] Maric D, Burrows JP. Analysis of the UV absorption spectrum of ClO: a comparative study of four methods for spectral computations. JQSRT 1999;62:345–69.
[101] Finlayson-Pitts BJ, Wingen LM, Sumner AL, Syomin D, Ramazan KA. The heterogeneous hydrolysis of NO_2 in laboratory systems and in outdoor and indoor atmospheres: an integrated mechanism. Phys Chem Chem Phys 2003;5(2):223–42.
[102] Stutz J, Kim ES, Platt U, Bruno P, Perrino C, Febo A. UV-Vis absorption cross-section of nitrous acid. J Geophys Res 2000;105:14,585–92.
[103] Platt U, New approaches of aromatic hydrocarbon measurements by DOAS. In: Proceedings of the Workshop Chemical Behaviour of Aromatic Hydrocarbons in the Troposphere, Valencia, 2000.
[104] Vandaele AC, Carleer M. Development of Fourier transform spectrometry for UV-visible differential optical absorption spectroscopy measurements of tropospheric minor constituents. Appl Opt 1999;38:2630–9.
[105] Volkamer R, Spietz P, Burrows JP. to be published.
[106] Chance KV, Hilsenrath E. Spectroscopic database needs for UV-VIS satellite measurements of atmospheric trace gases. NASA workshop on spectroscopic needs for atmospheric remote sensing, San Diego, 2001.
[107] Caspar C, Chance K. GOME wavelength calibration using solar and atmospheric spectra. In: Guyenne T-D, Danesy D, editors. Proceedings of the Third ERS Symposium on Space at the Service of our Environment, European Space Agency Special Publication SP-414, Noordwijk: ESTEC, 1997.
[108] Chance K. Analysis of BrO measurements from the global ozone monitoring experiment. Geophys Res Lett 1998;25:3335–8.
[109] Jenouvrier A, Coquart B, Merienne MF. Long pathlength measurements of oxygen absorption cross sections in the wavelength region 205–240 nm. JQSRT 1986;36:349–54.
[110] Yoshino K, Cheung AS-C, Esmond JR, Parkinson WH, Freeman DE, Guberman SL, Jenouvrier A, Coquart B, Merienne M-F. Improved absorption cross-sections of oxygen in the wavelength region 205–240 nm of the Herzberg continuum. Planet Space Sci 1988;36:1469–75.